論文 / 著書情報
Article / Book Information

Title	Ultra-high channel-count wavelength demultiplexer based on a Bragg reflector waveguide with large angular dispersion
Authors	Xiaodong Gu, Toshikazu Shimada, Akihiro Matsutani, Fumio Koyama
Citation	OPTICS EXPRESS, vol. 20, no. 26, B331-338
Pub. date	2012, 12
Copyright	Copyright (c) 2012 Optical Society of America

Ultra-high channel-count wavelength demultiplexer based on a Bragg reflector waveguide with large angular dispersion

Xiaodong Gu,[1,*] Toshikazu Shimada,[1] Akihiro Matsutani,[2] and Fumio Koyama[1]

[1]*Photonics Integration System Research Center, Precision and Intelligence Laboratory, Tokyo Institute of Technology, 4259-R2-22, Nagatsuta-cho, Midori-ku, Yokohama, 226-8503, Japan*
[2]*Semiconductor and MEMS Processing Center, Technical Department, Tokyo Institute of Technology, 4259-R2-3, Nagatsuta-cho, Midori-ku, Yokohama, 226-8503, Japan*
[*]*gu.xiaodong@ms.pi.titech.ac.jp*

Abstract: We present a new type of wavelength demultiplexers based on a Bragg reflector waveguide, which provides a large angular dispersion of 1~2°/nm. Benefiting from its large steering bandwidth and sharp divergence angles, we record a number of resolution-points (possible channel-count in demultiplexing) over 200 and 1,000 for active-type and passive-type devices, respectively. It is the highest number in various multiplexing elements ever reported. The device size is as small as a few millimeters.

OCIS codes: (130.3120) Integrated optics devices; (130.4815) Optical switching devices; (060.4230) Multiplexing.

References and links

1. C. A. Brackett, "Dense wavelength division multiplexing networks: principles and applications," IEEE J. Sel. Areas Comm. **8**(6), 948–964 (1990).
2. S. Tibuleac and M. Filer, "Transmission impairments in DWDM networks with reconfigurable optical add-drop multiplexers," J. Lightwave Technol. **28**(4), 557–598 (2010).
3. J. Tsai and M. C. Wu, "A high port-count wavelength-selective switch using a large scan-angle, high fill-factor, two-axis mems scanner array," IEEE Photon. Technol. Lett. **18**(13), 1439–1441 (2006).
4. M. Shirasaki, "Chromatic-dispersion compensator using virtually imaged phased array," IEEE Photon. Technol. Lett. **9**(12), 1598–1600 (1997).
5. G. H. Lee, S. Xiao, and A. M. Weiner, "Optical dispersion compensator with >4000-ps/nm tuning range using a virtually imaged phased array (VIPA) and spatial light modulator (SLM)," IEEE Photon. Technol. Lett. **18**(17), 1819–1821 (2006).
6. D. R. Wisely, "32 channel WDM multiplexer with 1-nm channel spacing and 0.7-nm bandwidth," Electron. Lett. **27**(6), 520–521 (1991).
7. M. Shirasaki, "Large angular dispersion by a virtually imaged phased array and its application to a wavelength demultiplexer," Opt. Lett. **21**(5), 366–368 (1996).
8. M. K. Smit, "New focusing and dispersive planar component based on an optical phased array," Electron. Lett. **24**(7), 385–386 (1988).
9. H. Takahashi, S. Suzuki, K. Kato, and I. Nishi, "Arrayed-waveguide grating for wavelength division multi/demultiplexer with nanometre resolution," Electron. Lett. **26**(2), 87–88 (1990).
10. K. Takada, M. Abe, T. Shibata, and K. Okamoto, "1-GHz-spaced 16-channel Arrayed-Waveguide grating for a wavelength reference standard in DWDM Network Systems," J. Lightwave Technol. **20**(5), 850–853 (2002).
11. K. Seno, K. Suzuki, N. Ooba, K. Watanabe, M. Ishii, H. Ono, and S. Mino, "Demonstration of channelized tunable optical dispersion compensator based on arrayed-waveguide grating and liquid crystal on silicon," Opt. Express **18**(18), 18565–18579 (2010).
12. D. Sinefeld, C. R. Doerr, and D. M. Marom, "A photonic spectral processor employing two-dimensional WDM channel separation and a phase LCoS modulator," Opt. Express **19**(15), 14532–14541 (2011).
13. P. Yeh, A. Yariv, and E. Marom, "Theory of Bragg Fiber," J. Opt. Soc. Am. **68**(9), 1196–1201 (1978).
14. X. Gu, T. Shimada, and F. Koyama, "Giant and high-resolution beam steering using slow-light waveguide amplifier," Opt. Express **19**(23), 22675–22683 (2011).
15. X. Gu, T. Shimada, A. Fuchida, A. Matsutani, A. Imamura, and F. Koyama, "Beam steering in GaInAs/GaAs slow-light Bragg reflector waveguide amplifier," Appl. Phys. Lett. **99**(21), 211107 (2011).
16. F. Koyama, "Recent advances of VCSEL photonics," J. Lightwave Technol. **24**(12), 4502–4513 (2006).

#177285 - $15.00 USD Received 2 Oct 2012; revised 9 Nov 2012; accepted 9 Nov 2012; published 29 Nov 2012

17. X. Gu, T. Shimada, A. Matsutani, and F. Koyama, "Miniature nonmechanical beam deflector based on Bragg reflector waveguide with a number of resolution points larger than 1000," IEEE Photonics J. **4**(5), 1712–1719 (2012).
18. G. Hirano and F. Koyama, "Slowing light in Bragg reflector waveguide with tilt coupling scheme," presented at 20th Annual Meeting of The IEEE Laser and Electro-Optical Society, LEOS2007, **MK1**, Florida, U.S.A., 21–25 Oct. 2007.
19. G. Lenz, E. Baruch, and J. Salzman, "Polarization discrimination properties of Bragg-reflection waveguides," Opt. Lett. **15**(22), 1288–1290 (1990).

1. Introduction

In dense wavelength division multiplexing (DWDM) systems [1], a high performance wavelength multiplexer/demultiplexer has played an important role in optical filters, wavelength selective switches, dispersion compensators, and other functional devices [2–6]. A diffraction grating [6] is the simplest component to realize these functions, however, its angular dispersion is not large enough (<0.05°/nm) so that a large number of channels are difficult to be obtained in a compact fashion. A virtually imaged phased array (VIPA) was proposed, increasing the angular dispersion by a factor of 10 to 20 [7]. However, the free spectrum range (FSR) of VIPA is rather small, which limits the optical bandwidth. Therefore, in order to increase the number of channels, a lot of elements are required. An arrayed waveguide grating (AWG) [8–10] is a high performance demultiplexer component but it has a tradeoff between angular dispersion and FSR. When an AWG is used as dispersion element in a free-space optics for dispersion compensators or spectral processors [11,12], the maximum number of channels is limited by the beam width radiated from the waveguide array end.

In this paper, a novel type of a wavelength demultiplexer based on a Bragg reflector waveguide [13,14] is presented. The angular dispersion of the device is further increased by a factor of 2 to 3 comparing with VIPA. In addition, the FSR can be over 100 nm. The device is similar to our previously reported beam steering device [14,15]. Its basic layer structure is the same as that of a vertical-cavity surface emitting laser (VCSEL) [16]. Well-established growth techniques offer a high-quality micro-cavity etalon. An epitaxial wafer with different design is used and the electrode pattern as well as fabrication process are modified for increasing the device resolution. The spectral resolution of the device is determined by the angular dispersion and the beam divergence angle. In our recent publication, the number of resolution-points, which is a figure of merits for beam-steering devices, exceeds 1,000 for 5 mm long devices [17]. This number also exhibits the ability to separate adjacent spectral lines for MUX/DEMUX devices in a fixed optical bandwidth. To our knowledge, it is the highest number ever reported for such compact devices. In this paper, we focus on some important device performances of our active and passive dispersion elements including their angular dispersion, crosstalk, resolutions and polarization dependences.

2. Device structure

The schematic view of the diffraction element based on a Bragg reflector waveguide is illustrated in Fig. 1 together with the top-view photo of one fabricated device. A schematic view of the whole demultiplexing system is also illustrated in Fig. 2. The Bragg reflector waveguide provides angular separation regarding wavelengths of input light. A cylindrical lens collimates the output in the lateral direction and the focusing lens converges the beam onto the receiver plane. We wish to realize as many distinguishable separating spots as possible to get a large potential channel number in this demultiplexer thanks to the large angular dispersion and large FSR.

#177285 - $15.00 USD Received 2 Oct 2012; revised 9 Nov 2012; accepted 9 Nov 2012; published 29 Nov 2012

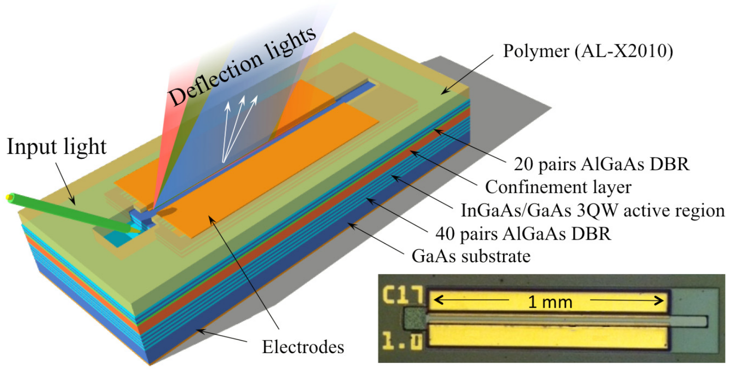

Fig. 1. Schematic view of a Bragg reflector waveguide diffraction element and a top-view photo of one fabricated device with a length of 1 mm.

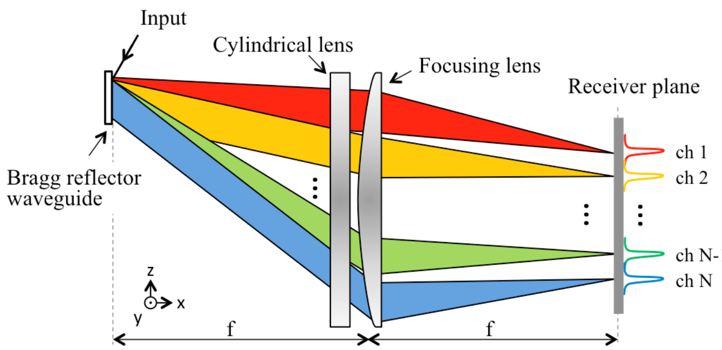

Fig. 2. Schematic view of a large channel-number demultiplexer based on the Bragg reflector waveguide.

The device consists of AlGaAs distributed Bragg reflectors (DBR) as top- and bottom-mirrors, a one-lambda active region with three InGaAs/GaAs quantum wells (3QW), an oxide confinement layer, and a GaAs substrate. The confinement structure is formed for lateral optical and current confinement. Besides that, polymer (AL-X2010, Asahi Glass) is patterned to protect the waveguide sidewall from current leakage and electrodes are used for current injection. While the operating wavelength band is around 980 or 990 nm in the present devices, it is flexible to change the wavelength band to other regions, e.g. 1310 or 1550 nm communication bands. It is because the device working scheme applies for any chip if it has a same layer structure as a VCSEL, of which the spectral range is extremely wide. An input light is coupled through a lensed fiber to the waveguide and travels along the waveguide as a 'slow-light mode'. Due to the insufficient reflectivity of the top-mirror, a portion of the light is radiated from the waveguide surface. Because the 'slow-light' travels in a zigzag way inside the waveguide, the device functions like a virtually-imaged grating with ultra-small emitter period and very low diffraction order. Therefore, light propagation in the waveguide is highly dispersive, i.e., the deflection angle changes largely if we tune the wavelength of input light. Details of the device operation principle have been reported in [14].

3. Active-type devices

We first fabricated an active-type Bragg reflector waveguide and tested its characteristics. A CCD camera is set above the device for capturing the far field patterns (FFPs) of the deflection beam. We measured the device with 50 mA current injection. Figures 3 (a) and 3(b) show the FFP images and intensity profiles, respectively. Continuous deflection angle change for input wavelength of 961 to 976 nm is obtained. The angle shifts over 20 degrees.

#177285 - $15.00 USD Received 2 Oct 2012; revised 9 Nov 2012; accepted 9 Nov 2012; published 29 Nov 2012

We are not able to keep the input power and polarization state constant of the applied external laser source, therefore, intensities of each wavelength are individually normalized. The actual intensity variation can be estimated from the coupling efficiency [14]. For an input wavelength longer than 976 nm, the coupling efficiency from fiber to slow-light mode is larger than 10dB. It is because the input fiber position and angle are fixed and optimized for shorter wavelengths. In simulation, 2dB coupling efficiency can be obtained optimally. Experimental demonstration has been reported previously in a similar device [18]. For those active-type devices, a device insertion loss can be fully compensated through current injection. In fact, even a positive device gain is possible after strong pumping to a long device. Although some additional noise, which mainly comes from the spontaneous emission, will be introduced from current injection, the intensity peak of FFP profile dramatically increases, much faster than the increase in noise level. Therefore, the signal noise ratio (SNR) is actually improved after pumping in the active-type device [15]. In addition, higher SNR can be obtained when the input wavelength is shifted away from the photo luminance peak, which can be confirmed from Fig. 3(b). We need to refrain from lasing in this VCSEL-like device, because a stimulated emission will deplete the active gain. At the moment, a lateral lasing happens first, thus, we need to design an absorption region or anti-reflection coating at the end of the waveguide, if we wish to pump harder. Alternatively, we are also able to design passive waveguides with extremely low propagation loss in order to get a sharper FFP profile and a high SNR. Although we cannot inject current into those waveguides, 5 times higher resolution can be obtained. The details will be discussed in Section 4. We fixed the polarization state of TE mode in the present experiment and the polarization dependence will also be discussed in Section 4.

The measured deflection angle is plotted together with numerical simulation results in Fig. 4. The results well agree with each other. The waveguide cutoff wavelength $\lambda_{\mathrm{cutoff}}$ here is approximately 982 nm. We also show the measured and calculated angular dispersion $\Delta\theta/\mathrm{d}\lambda$ in the same figure. An angular dispersion of 1~2°/nm is a very large number comparing with other dispersion components, to be discussed in Section 5.

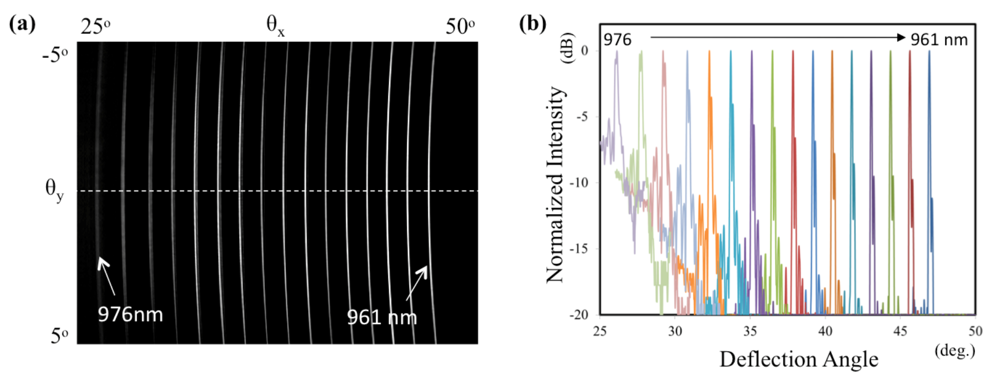

Fig. 3. (a) Far-field patterns and (b) intensity profiles on the receiver plane of the output. Input wavelength is from 961 to 976 nm, 50mA current is injected into the waveguide for compensating radiation loss. Cutoff wavelength is ~982 nm here.

#177285 - $15.00 USD Received 2 Oct 2012; revised 9 Nov 2012; accepted 9 Nov 2012; published 29 Nov 2012

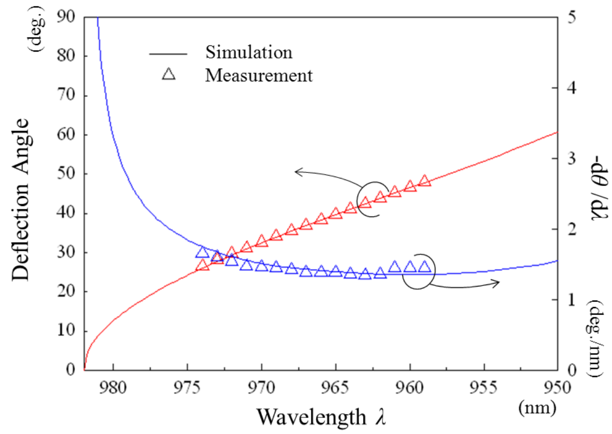

Fig. 4. Simulation and measurement results of the deflection angle and angular dispersion $\Delta\theta/\mathrm{d}\lambda$ as a function of input wavelength λ.

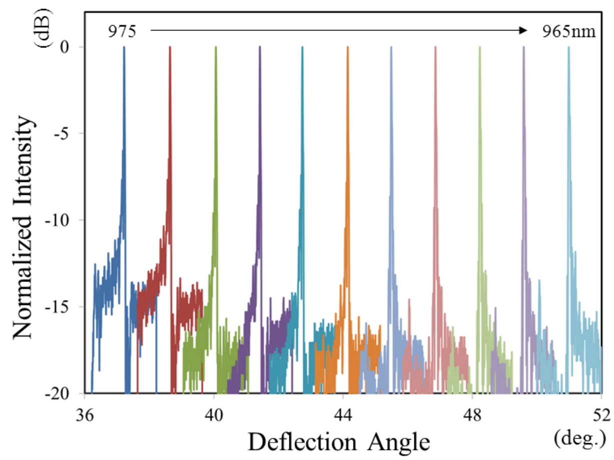

Fig. 5. Intensity profiles of FFP patterns for a passive-type device captured by a high-resolution measurement setup. Input wavelengths are from 965 to 975 nm. λ_{cutoff} is 990 nm here.

4. Passive-type devices

To further investigate the resolution potential in those Bragg reflector waveguides, we designed and fabricated a low-propagation-loss passive-type device [17]. The active region is replaced by a transparent bulk GaAs core, and the distributed Bragg reflector (DBR) multilayers are un-doped so as to reduce the material absorption. The pair numbers for the top- and bottom-DBR are 28 and 40. As a result, the slow-light propagation loss is dramatically reduced to 2~20 cm^{-1} for a wide wavelength range, which enables a long propagation distance (large beam width), resulting in an ultra-low output divergence angle. In Fig. 5, measured FFP profiles for a wavelength range from 965 to 975 nm are plotted for a TE mode input. The intensities are also individually normalized here. The length of the measured device is 5 mm. To be noted here, λ_{cutoff} in this passive-type device is 990 nm, which is about 8 nm longer than that of the active-type device, so the deflection angles are correspondingly shifted. A higher-resolution measurement setup with a resolution of below 0.004° incorporating with a collimator is applied, thus we could investigate the output beam profile and rejection ratio (crosstalk). Figure 6 shows the magnified FFP profile of a single-spectral line at 969 nm. Its full width at half maximum (FWHM) is as narrow as 0.028°. Some tails are found beside the main peaks. They are caused by the interference between the output

#177285 - $15.00 USD Received 2 Oct 2012; revised 9 Nov 2012; accepted 9 Nov 2012; published 29 Nov 2012

radiation and the reflection light at an input. It can explain why the tail shapes differ between left and right of the reflection angle (the input angle is ~45°). Here the SNR is 10~15dB for a large steering band. It can be improved by suppressing or blocking the reflection at the fiber coupling region and beginning part of the waveguide. Further sharpening the beam divergence can also largely increase the SNR. The coupling efficiency of passive-type devices is about the same to active-type chips. Its insertion loss is mainly determined by the coupling because the propagation loss is extremely low that most of the coupled energy is radiated as output.

Polarization dependence is also important in demultiplexing devices. If we look at the deflection angle difference between the TE- and TM-polarized inputs, as illustrated in Fig. 7, the current device exhibits a value of 0.5°~1.5°. It is caused by the difference in penetration lengths in DBRs for the two polarization states [19]. If we make minor modification to the core thickness, we are able to decrease this θ_{TE}-θ_{TM}. The design value of the device in the present experiment is 0.29 µm. In simulation, by decreasing the core thickness to 0.2795 µm in epitaxial growth, $|\theta_{TE}-\theta_{TM}|$ can be smaller than 0.05° for the whole wavelength band, which is corresponding to a wavelength separation of around 0.05nm.

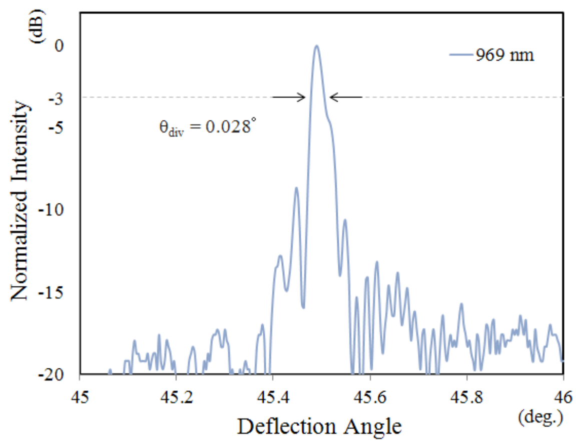

Fig. 6. Intensity profile of FFP pattern for a single-spectral line at 969 nm.

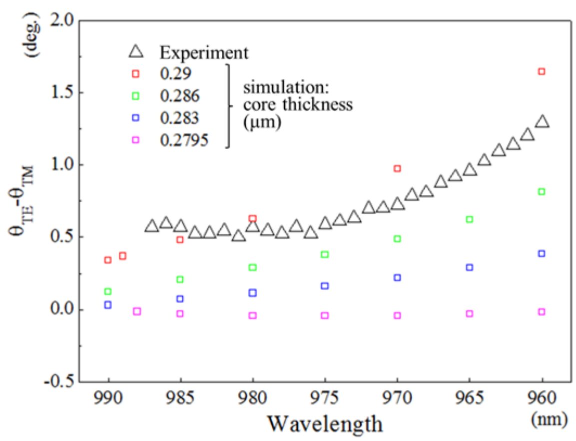

Fig. 7. Deflection angle difference between two polarization states at different wavelengths. Simulations and experiment results for various core thicknesses are compared.

#177285 - $15.00 USD Received 2 Oct 2012; revised 9 Nov 2012; accepted 9 Nov 2012; published 29 Nov 2012

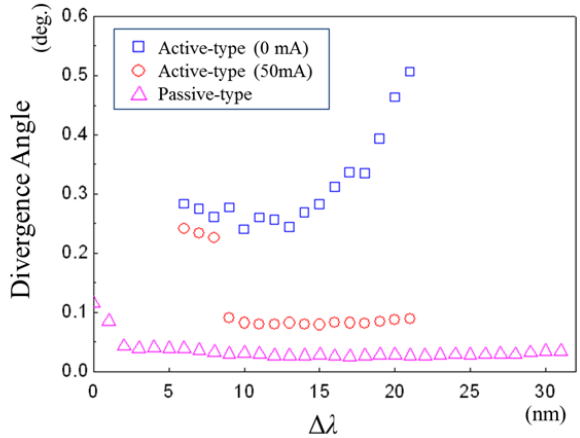

Fig. 8. Divergence angle versus wavelength for different current injections in the active-type devices and 5 mm long passive-type device.

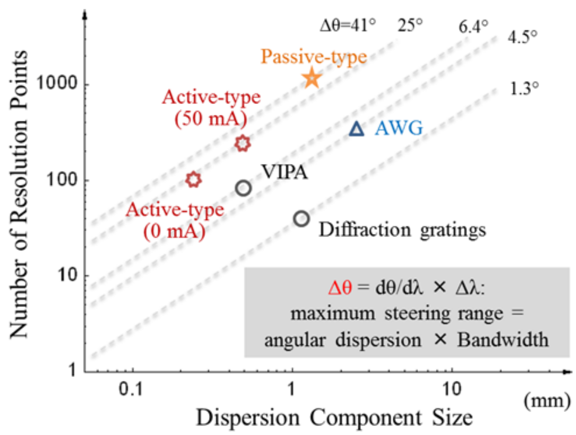

Fig. 9. A summary of different dispersion elements.

5. Discussions

Figure 8 shows the divergence angle versus wavelength for different current injections in the active-type and passive-type devices. The divergence angle can be directly obtained from the full width at half maximum (FWHM) of the FFP intensity profile, which has an x-axis of deflection angles. An obvious improvement can be seen after pumping 50 mA to the active-type device while a further improvement is obtained in the passive-type device. The number of resolution-points *N*, defined as steering range divided by divergence angle, exhibits the device's ability to separate adjacent spectral lines in a fixed optical bandwidth. It can be viewed as the channel number shown in the receiver plane in Fig. 2.

The resolution numbers for dispersion elements are summarized in Fig. 9. We wish to get as large N as possible. If we look at the maximum steering angle $\Delta\theta$, which is the product of angular dispersion $d\theta/d\lambda$ and optical bandwidth $\Delta\lambda$, our proposed device shows distinguished performance over other approaches. Diffraction grating has very low $d\theta/d\lambda$ of smaller than 0.05°/nm, and hence $\Delta\theta$ is limited. For VIPA, $d\theta/d\lambda$ can be increased by over 10 times, but $\Delta\lambda$ is strictly limited by FSR. From Fig. 4, we could see the proposed device has $d\theta/d\lambda$ of 1~2°/nm, doubling that of VIPA. In addition, due to its large FSR of over 100 nm, $\Delta\theta$ is determined by the optical bandwidth. In active-type devices, $\Delta\theta$ over 20° range is obtained while $\Delta\theta$ over 40° is demonstrated in passive-type devices. As a result, *N* of the active-type devices with and without current injection are ~200 and ~80, respectively. Furthermore, an *N*

#177285 - $15.00 USD Received 2 Oct 2012; revised 9 Nov 2012; accepted 9 Nov 2012; published 29 Nov 2012

over 1,000 is successfully recorded because a maximum divergence angle is below 0.04° within a certain tuning band ($\Delta\lambda$ = 30 nm). We believe it is the largest value ever reported for those dispersive elements. Moreover, the device size is still kept in millimeter-order even for reaching such a high resolution thanks to the angular dispersion and large FSR.

6. Conclusion

We designed and fabricated a novel type of a wavelength demultiplexer based on a Bragg reflector waveguide. It exhibits a large angular dispersion of 1~2°/nm. We realized a high number of resolution-points N over 200 for 1 mm long active-type device by compensating the propagation loss by current injection. Furthermore, an N exceeding 1,000 is achieved in a 5 mm long low-loss passive-type device. The proposed concept may offer a large-scale optical routing and switching building block in compact fashion for DWDM systems.

Acknowledgment

This work was supported by Grant-in-Aid for Scientific Research (S) from the Ministry of Education, Culture, Sports, Science and Technology of Japan (#22226008).